

Gapless topological Fulde-Ferrell superfluidity induced by in-plane Zeeman field

Hui Hu¹, Lin Dong², Ye Cao¹, Han Pu², and Xia-Ji Liu¹

¹*Centre for Quantum and Optical Science, Swinburne University of Technology, Melbourne 3122, Australia and*

²*Department of Physics and Astronomy, and Rice Quantum Institute, Rice University, Houston, TX 77251, USA*

(Dated: April 10, 2014)

Topological superfluids are recently discovered quantum matters that host topologically protected gapless edge states known as Majorana fermions - exotic quantum particles that act as their own anti-particles and obey non-Abelian statistics. Their realizations are believed to lie at the heart of future technologies such as fault-tolerant quantum computation. To date, the most efficient scheme to create topological superfluids and Majorana fermions is based on the Sau-Lutchyn-Tewari-Das Sarma model with a Rashba-type spin-orbit coupling on the x - y plane and a large out-of-plane (perpendicular) Zeeman field along the z -direction. Here we propose an alternative setup, where the topological superfluid phase is driven by applying an in-plane Zeeman field. This scheme offers a number of new features, notably Cooper pairings at finite centre-of-mass momentum (i.e., Fulde-Ferrell pairing) and gapless excitations in the bulk. As a result, a novel gapless topological quantum matter with inhomogeneous pairing order parameter appears. It features unidirected Majorana surface states at boundaries, which propagate in the same direction and connect two Weyl nodes in the bulk. We demonstrate the emergence of such an exotic topological matter and the associated Majorana fermions in spin-orbit coupled atomic Fermi gases and determine its parameter space. The implementation of our scheme in semiconductor/superconductor heterostructures is briefly discussed.

PACS numbers: 05.30.Fk, 03.75.Hh, 03.75.Ss, 67.85.-d

The possibility of realizing topological superfluids and manipulating Majorana fermions in solid-state and ultracold atomic systems is currently a topic of great theoretical and experimental interest [1, 2], due to their potential applications in fault-tolerant topological quantum computation [3]. Roughly, Majorana fermions constitute “half” of an ordinary Dirac fermion, in the sense that two real Majorana fermions γ_1 and γ_2 - which can be separated in arbitrary distance - mathematically define a complex fermion operator $c = \gamma_1 + i\gamma_2$ [4]. The exchange statistics of Majorana fermions is exotic. Unlike conventional bosons and fermions, braiding Majorana fermions around one another in a 2^N -dimensional Hilbert space (spanned by $2N$ well-separated Majorana fermions) produce non-Abelian unitary transformations in the Hilbert space. Quantum information can then be non-locally encoded in the Hilbert space by such braiding operators and be immune to decoherence, which is ideal for the purpose of quantum computation [3].

At present, a number of experimental settings have been suggested for hosting Majorana fermions under appropriate conditions, including chiral p -wave superconductors [5], fractional quantum Hall systems at filling $\nu = 5/2$ [6], and topological insulators or semiconductor nanowires in proximity to an s -wave superconductor [7–9]. The latest setting, which seems to be the most practical setup, is described by the Sau-Lutchyn-Tewari-Das Sarma (SLTD) model [8]. The key idea of this mechanism is that the Fermi surfaces are spin-split by a Rashba spin-orbit coupling on the x - y plane and a perpendicular out-of-plane Zeeman field along the z -direction. If the number of

particles is tuned to make the inner Fermi surface disappear, the superconductivity will be only induced by pairing on the outer Fermi surface, which is of p -wave in nature [10, 11], and therefore becomes topologically nontrivial. Following this promising theoretical model, exciting experimental progress for the observation of Majorana fermions has been made very recently [12–14], although unambiguous confirmation for their existence still remains elusive.

The SLTD mechanism uses an out-of-plane Zeeman field to split the Fermi surfaces [8]. It is interesting that such a splitting can also be achieved by applying a large in-plane Zeeman field in combination with spin-orbit coupling, as illustrated in Fig. 1. Furthermore, the in-plane field together with spin-orbit coupling is known to introduce an asymmetry in the single-particle dispersion [15, 16], consequently to induce Cooper pairs with nonzero centre-of-mass momentum [17–24] and hence realize the so-called spatially inhomogeneous Fulde-Ferrell (FF) pairing scenario [25]. It is therefore of interest to ask whether a topological phase transition can also be driven by an in-plane Zeeman field only? If the answer is yes, then we must be able to observe an exotic inhomogeneous topological FF superfluid that supports Majorana fermions. The understanding of such a new-type topological state of matter may greatly enrich our knowledge about topological superfluids.

In this work, we examine the new mechanism by using an ultracold atomic setting of a three-dimensional (3D) spin-orbit coupled atomic Fermi gas subject to an in-plane Zeeman field. By increasing the field strength

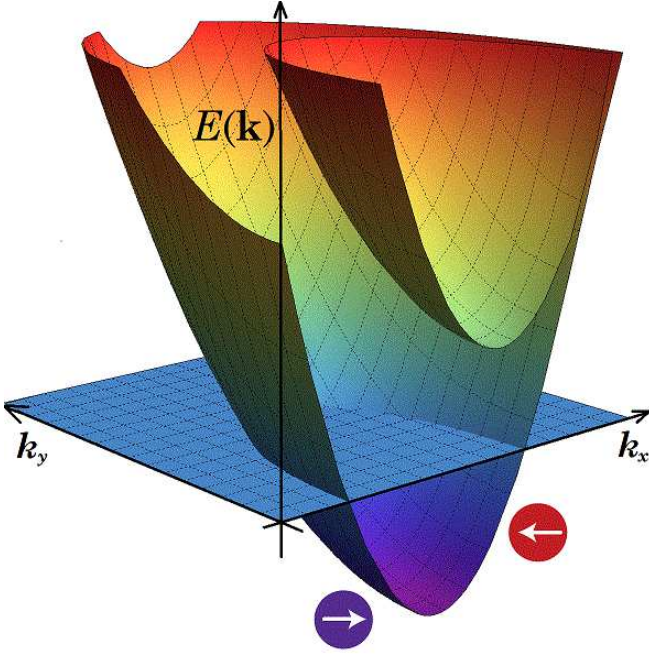


FIG. 1: (Color online). **Formation of an effective p -wave energy band.** The energy band of the system splits into two by spin-orbit coupling. A large in-plane Zeeman field along the x -direction strongly tilts the energy dispersion. When the Fermi energy lies below the upper band, atoms occupy the lower band only and form an effective “spinless” system, in which the new composite particle consists of both spin-up and spin-down ingredients (shown by circles with arrows) and interacts with each other via an effective p -wave interaction.

above a threshold, we observe the change of the topology of the Fermi surfaces that triggers a topological phase transition. The resulting inhomogeneous topological FF superfluid is gapless in the bulk with nodal points form closed surfaces in momentum space. While in real space, it hosts unidirected Majorana surface states that propagate in the same direction at boundary. These unique features are absent in standard topological superfluids known so far such as the p -wave superconductors or the SLTD-type superconductors, both of which are gapped in the bulk and support counter-propagating Majorana modes at surfaces. We find that the phase space for the proposed novel gapless topological FF superfluid is significant, implying that it could be easily realized in current ultracold atomic experiments owing to the unprecedented tunability of synthetic spin-orbit coupling, Zeeman field and interatomic interaction in cold-atom laboratory [26–28]. We also discuss briefly the potential implementation of our proposal in solid-state setups.

Results. — For concreteness, we focus on a 3D spin-orbit coupled two-component Fermi gas with an isotropic spin-orbit coupling $V_{SO}(\hat{\mathbf{k}}) = \lambda(\hat{k}_x\sigma_x + \hat{k}_y\sigma_y + \hat{k}_z\sigma_z)$ subject to an in-plane Zeeman field $h\sigma_x$ [20, 29, 30], which

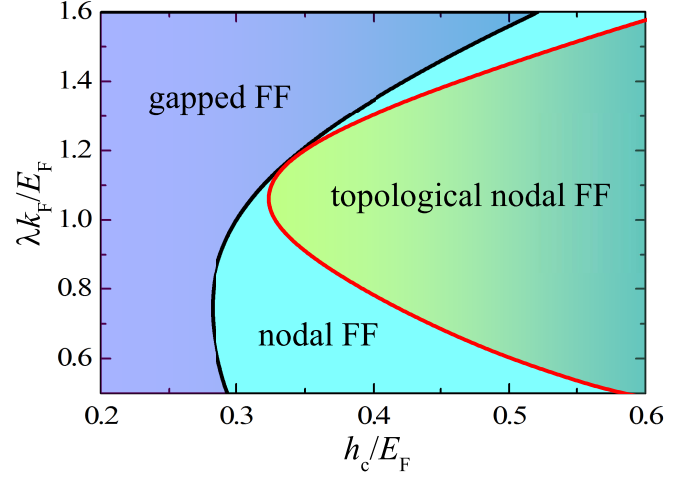


FIG. 2: (Color online) **Zero temperature phase diagram of the FF superfluid at the interaction parameter $1/(k_F a_s) = -0.5$.** With increasing the in-plane Zeeman field, the Fermi cloud changes from a gapped FF superfluid to a gapless FF superfluid, and finally turns into a gapless topological superfluid.

can be described by the model Hamiltonian,

$$\mathcal{H} = \int d\mathbf{r} \left[\sum_{\sigma\sigma'} \psi_{\sigma}^{\dagger}(\mathbf{r}) H_0^{\sigma\sigma'} \psi_{\sigma'}(\mathbf{r}) + \mathcal{V}_{int} \right], \quad (1)$$

where $\psi_{\sigma}^{\dagger}(\mathbf{r})$ (ψ_{σ}) is the field operator for creating (annihilating) an atom with pseudo-spin state $\sigma \in (\uparrow, \downarrow)$ at position \mathbf{r} , $H_0 = -\hbar^2 \nabla^2 / (2m) - \mu + V_{SO}(\hat{\mathbf{k}}) + h\sigma_x$ is the single-particle Hamiltonian with the atomic mass m and chemical potential μ , $\hat{k}_{i=(x,y,z)} = -i\partial_i$ is the momentum operator and $\sigma_{x,y,z}$ are the Pauli matrices. $\mathcal{V}_{int} = U_0 \psi_{\uparrow}^{\dagger}(\mathbf{r}) \psi_{\downarrow}^{\dagger}(\mathbf{r}) \psi_{\downarrow}(\mathbf{r}) \psi_{\uparrow}(\mathbf{r})$ describes a pairwise attractive contact interaction of strength $U_0 < 0$, where $U_0^{-1} = m / (4\pi \hbar^2 a_s) - V^{-1} \sum_{\mathbf{k}} m / (\hbar^2 \mathbf{k}^2)$ can be expressed in terms of the s -wave scattering length a_s . At the mean-field level, the model Hamiltonian can be solved by taking an order parameter $\Delta(\mathbf{r}) = -U_0 \langle \psi_{\downarrow}(\mathbf{r}) \psi_{\uparrow}(\mathbf{r}) \rangle$ and linearizing the interaction Hamiltonian $\mathcal{V}_{int} \simeq -[\Delta(\mathbf{r}) \psi_{\uparrow}^{\dagger}(\mathbf{r}) \psi_{\downarrow}^{\dagger}(\mathbf{r}) + \text{H.c.}] - |\Delta(\mathbf{r})|^2 / U_0$.

In the presence of an in-plane Zeeman field $h\sigma_x$, it is now widely understood that Cooper pairs acquire a finite centre-of-mass momentum $\mathbf{Q} = q\mathbf{e}_x$ along the x -direction, i.e., $\Delta(\mathbf{r}) = \Delta e^{iqx}$ [15, 17–20]. By using the Nambu spinor $\Phi(\mathbf{r}) \equiv [\psi_{\uparrow} e^{iqx/2}, \psi_{\downarrow} e^{iqx/2}, \psi_{\uparrow}^{\dagger} e^{-iqx/2}, \psi_{\downarrow}^{\dagger} e^{-iqx/2}]^T$ to gauge out the momentum related phase in the order parameter, the mean-field model Hamiltonian can be solved by diagonalizing the following Bogoliubov-de Gennes (BdG) Hamiltonian

$$\mathcal{H}_{BdG}(\hat{\mathbf{k}}) \equiv \begin{bmatrix} H_0 \left(\frac{\mathbf{Q}}{2} + \hat{\mathbf{k}} \right) & -i\Delta\sigma_y \\ i\Delta\sigma_y & -H_0^* \left(\frac{\mathbf{Q}}{2} - \hat{\mathbf{k}} \right) \end{bmatrix}, \quad (2)$$

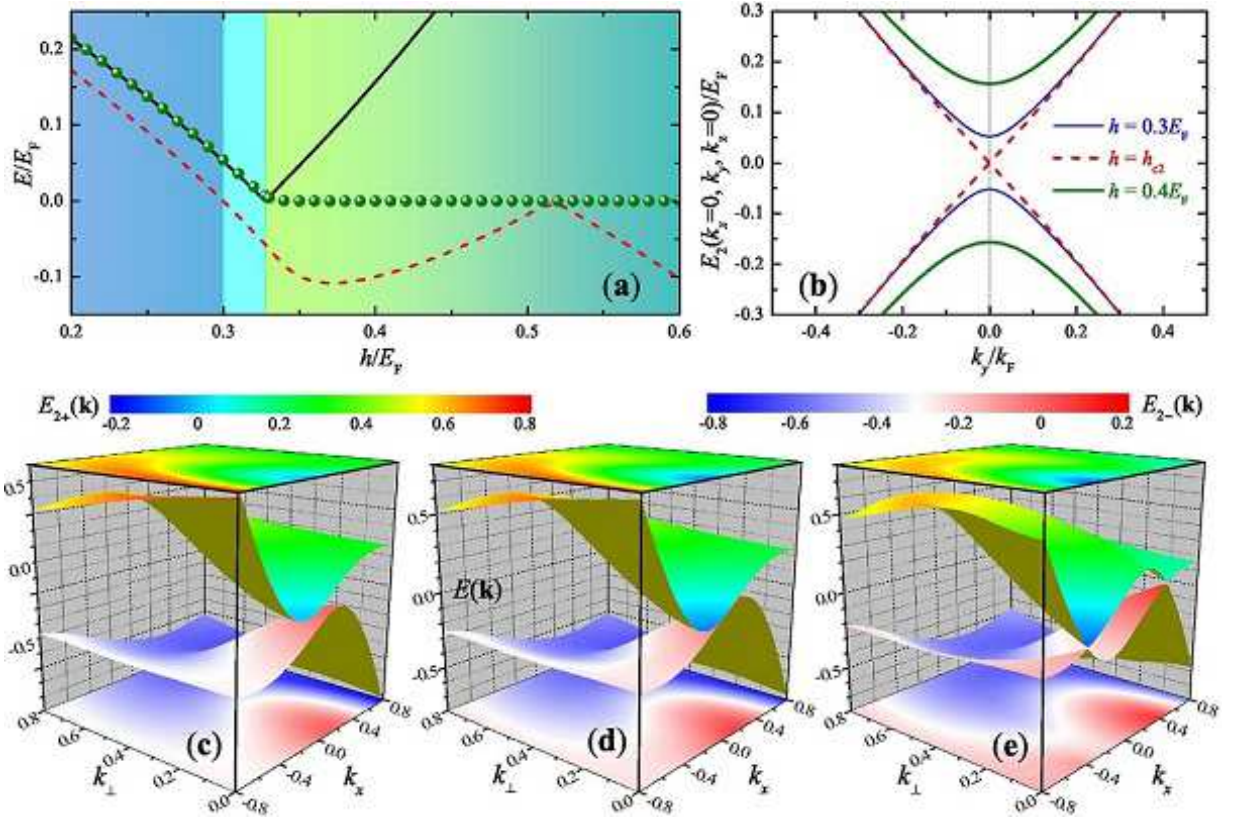


FIG. 3: (Color online) **The evolution of the energy gap and of the topology of the Fermi surfaces at $\lambda = E_F/k_F$ with increasing in-plane Zeeman field.** (a) The global energy gap $E_g = \min E_{2+}(\mathbf{k})$ (red dashed line), the energy gap at $\mathbf{k} = 0$ (black solid line), and the minimum energy of the surface states (green solid circles) when open boundary is imposed to the y - z plane. (b) The energy dispersion $E_{2\pm}(k_y)$ at $k_x = 0$ and $k_z = 0$. (c), (d) and (e) The 3D full plot of the energy dispersion $E_{2\pm}(k_x, k_\perp = \sqrt{k_y^2 + k_z^2})$ at $h_{c1} \simeq 0.3E_F$ (c), $h_{c2} \simeq 0.327E_F$ (d) and $h = 0.4E_F$ (e).

i.e., $\mathcal{H}_{BdG}\Phi_{\mathbf{k}\eta}^\nu(\mathbf{r}) = E_{\eta\nu}(\mathbf{k})\Phi_{\mathbf{k}\eta}^\nu(\mathbf{r})$, which gives rise to the wavefunction of Bogoliubov quasiparticles, $\Phi_{\mathbf{k}\eta}^\nu(\mathbf{r}) = 1/\sqrt{V}e^{i\mathbf{k}\cdot\mathbf{r}}[u_{\eta\uparrow}^\nu, u_{\eta\downarrow}^\nu, v_{\eta\uparrow}^\nu, v_{\eta\downarrow}^\nu]^T$, and the energy $E_{\eta\nu}(\mathbf{k})$. We obtain four quasi-particle energy dispersions, indexed by $\nu \in (+, -)$ for the particle (+) or hole (-) branch, and $\eta \in (1, 2)$ for the upper (1) or lower (2) helicity band split by spin-orbit coupling. We derive the gap and number equations from the resulting mean-field thermodynamic potential (see Methods) and solve them self-consistently to obtain Δ , q and μ , from which we determine the phase diagram at zero temperature, as reported in Fig. 2. In our numerical calculations, using the number density n we have set the Fermi wavevector $k_F = (3\pi^2n)^{1/3}$ and Fermi energy $E_F = \hbar^2k_F^2/(2m)$ as the units for wavevector and energy, respectively. Unless specifically noted, we shall focus on the weak coupling case with a dimensionless interaction parameter $1/(k_F a_s) = -0.5$ and at zero temperature $T = 0$, for which our mean-field treatment could be well justified.

It is readily seen from the phase diagram that an in-plane Zeeman field will drive the Fermi system from a gapped FF superfluid to a gapless phase (labelled as “nodal FF”) [20]. Remarkably, at sufficiently large value

it will also lead to a gapless topologically non-trivial state (“topological nodal FF”). The evolution of the energy spectrum at a typical spin-orbit coupling strength $\lambda = E_F/k_F$ as a result of the increasing in-plane Zeeman field is presented in Fig. 3.

Physically, the transition to a gapless phase can be well characterized by a global energy gap $E_g = \min E_{2+}(\mathbf{k})$, which is the half of the energy difference between the minimum energy of the particle branch and the maximum of the hole branch due to the particle-hole symmetry $E_{2+}(\mathbf{k}) = -E_{2-}(-\mathbf{k})$. Hence, $E_g \leq 0$ and $E_g > 0$ characterize a gapless and gapped state, respectively. The topological phase transition, on the contrary, is related to the change of the topology of the Fermi surfaces. It is well known that such a change must be accompanied with the close and re-open of an energy gap at some specific points in momentum space [1, 2]. In our continuum case of a homogeneous Fermi gas, this occurs precisely at the origin $\mathbf{k} = \mathbf{0}$ (see Fig. 3b). Therefore, naively the topological transition can be determined from the condition

$E_{2+}(\mathbf{k} = \mathbf{0}) = 0$ or more explicitly,

$$h_{c2} = \sqrt{\left(\mu - \frac{\hbar^2 q^2}{8m}\right)^2 + \Delta^2} - \frac{\lambda q}{2}. \quad (3)$$

In the absence of an FF pairing momentum ($q = 0$), the above condition reduces to the well-known criterion $h_c = \sqrt{\mu^2 + \Delta^2}$ for the appearance of an SLTD topological superfluid when an out-of-plane Zeeman field is applied [8, 9]. It is interesting that the gapless transition always occurs before the topological transition, as a result of $E_g \leq E_{2+}(\mathbf{k} = \mathbf{0})$. Thus, bulk-gapped topological FF superfluids, if exist, must appear at very high in-plane Zeeman field. As a superfluid analogue of strong 3D topological insulators [1, 2], they are anticipated to have the unique feature of a single Dirac cone for the energy dispersion of the Majorana edge states. Unfortunately, in the parameter space that we considered, we do not find their existence.

At the coupling strength $\lambda = E_F/k_F$, the gapless transition and topological transition occur at $h_{c1} \simeq 0.3E_F$ and $h_{c2} \simeq 0.327E_F$, respectively, as can be seen from Fig. 3a, where E_g (red dashed line) and $E_{2+}(\mathbf{k} = \mathbf{0})$ (black solid line) become zero as the in-plane Zeeman field increases. When $h > h_{c1}$, nodal points which satisfy $E_{2\pm}(\mathbf{k}) = 0$ develop and form two closed surfaces in momentum space [20]. When the in-plane field further increases, passing through the threshold h_{c2} for the topological transition (see Fig. 3d), the energy dispersions of the particle- and hole-branches touch at two specific points ($\pm k_W, 0, 0$), as shown in Fig. 3e. Around these points, the dispersion of Bogoliubov quasiparticles in the bulk acquires a linear structure and thereby form a Dirac cone. This is precisely the energy dispersion for massless Weyl fermions [31–33]. In this sense, the gapless topological FF superfluid predicted in this work provides a new avenue for the observation of Weyl fermions around the Weyl nodes ($\pm k_W, 0, 0$). Indeed, Weyl fermions have recently been discussed in the context of 3D gapped topological superfluids [34, 35].

In our case, the appearance of the Weyl nodes and of the topological order is closely related. Due to the asymmetry in the k_x axis, only one of the Weyl nodes is occupied. Thus, we may characterize the topological order of the gapless FF superfluid by using the topological invariant of Weyl fermions [2, 36]:

$$N_W = \int \frac{d^3\mathbf{k}}{24\pi^2} \epsilon^{\mu\nu\rho} \text{Tr} \left[Q_{\mathbf{k}}^\dagger \partial_\mu Q_{\mathbf{k}} Q_{\mathbf{k}}^\dagger \partial_\nu Q_{\mathbf{k}} Q_{\mathbf{k}}^\dagger \partial_\rho Q_{\mathbf{k}} \right], \quad (4)$$

where $Q_{\mathbf{k}}$ is the unitary matrix determined by the BdG Hamiltonian, $\mu, \nu, \rho = (k_x, k_y, k_z)$ and the domain of the integration includes the isolated, occupied Weyl node. The gapless topological FF superfluid is uniquely characterized a nonzero topological invariant $N_W \neq 0$.

To further demonstrate the topological nature of the gapless FF superfluid, we calculate the energy dispersion

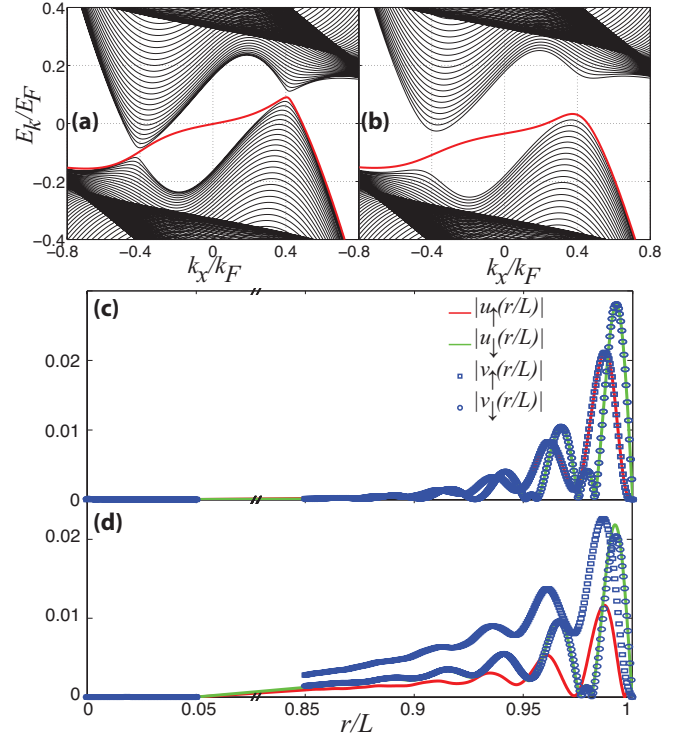


FIG. 4: (Color online) **Majorana surface states arising from the hard wall confinement perpendicular to the y - z plane.** (a) and (b) The energy spectrum $E_{k_x}^{(m)}$ as a function of k_x for $m = 0$ and $m = 10$, respectively. (c) The wavefunction of the zero-energy Majorana fermions for $m = 0$, satisfying the symmetry $u_\sigma(r) = e^{i\vartheta} v_\sigma^*(r)$, where ϑ is a constant phase factor and $\sigma = \uparrow, \downarrow$. (d) The wavefunction of the zero-energy surface state for $m = 10$. In numerical calculations, we have set the radius of the confinement $L = 200k_F^{-1}$. Other parameters are $\lambda = E_F/k_F$ and $h = 0.4E_F$.

in the presence of open boundary by imposing cylindrical hard wall confinement perpendicular to the y - z plane with the x -axis being the symmetry axis (see Methods). There is a pair of zero-energy Majorana fermion state on the boundary of $r = \sqrt{y^2 + z^2} = L$, which is the direct signature of a topologically non-trivial state. The existence of Majorana fermions is reported in Fig. 3a by green solid circles. They immediately appear after the change in the topology of the Fermi surfaces.

We now discuss in more detail the Majorana surface states, whose dispersion is shown in Fig. 4. Because the boundary we impose has cylindrical symmetry in the y - z plane and translational symmetry along the x -direction, the quasiparticle wavefunction takes the following form:

$$\Phi_{k_x\eta}^\nu = e^{ik_x x} e^{im\phi} [u_{\eta\uparrow}^\nu(r), u_{\eta\downarrow}^\nu(r) e^{i\phi}, v_{\eta\uparrow}^\nu(r) e^{i\phi}, v_{\eta\downarrow}^\nu(r)]^T, \quad (5)$$

where (x, r, ϕ) form the cylindrical coordinates. States with different orbital angular momentum quantum number m and linear momentum k_x are decoupled, see Methods for basis expansion. In Figs. 4a and 4b, we plot the

energy spectrum along k_x axis for $m = 0$ and $m = 10$, respectively. Majorana zero energy mode can be identified by the energy crossing of surface state contribution, at which points quasiparticle wavefunctions become localized near the boundary $r = L$, as shown in Figs. 4c and 4d. The surface states smoothly connect to the Weyl nodes located approximately at $k_W \simeq 0.4k_F$ in the bulk. As $|m|$ increases, the localization of the zero-energy surface modes deteriorates due to their hybridization with the bulk modes, and the desired symmetry $u_\sigma(r) = e^{i\vartheta} v_\sigma^*(r)$ ($\sigma = \uparrow, \downarrow$) for Majorana mode [37] is violated (see Fig. 4d). One can prove that, as a result of particle-hole symmetry of the BdG equation, when $m \rightarrow -m - 1$, and $k_x \rightarrow -k_x$, we have $E_{\eta\nu} \rightarrow -E_{\eta\nu}$. Hence for every zero-energy state at given m and k_x , there is a corresponding zero-energy state at $-m - 1$ and $-k_x$, which describes the same physical state. As a result, it is easy to see from Figs. 4a and 4b that for arbitrary azimuthal angular momentum m , the Majorana surface states have nearly the same unidirected velocity $v(k_x) = \partial E_{k_x}^{(m)} / \partial k_x > 0$. As there are no net atomic currents at equilibrium, the current carried by these co-propagating surface states must be compensated by the current induce by some extra counter-propagating modes in the bulk. This is only possible when the system is gapless in the bulk, consistent with the gapless nature of our topological FF superfluid. The unidirected surface states discussed in our work is therefore a unique feature of novel gapless topological FF superfluid.

We may also consider imposing hard wall confinement along a specific direction, for example, along the y -direction at $y = 0, L$. In this case, unidirected Majorana surface states propagate in the same direction on opposite boundaries at $y = 0$ and $y = L$, respectively. For detailed discussions, we refer to Supplementary Information.

It is worth noting that the 3D gapless topological FF superfluid can not be viewed as a stack of 2D topological superfluids along a specific direction (i.e., z -axis), unlike the standard 3D topological superfluids known so far. For the latter, the Majorana surface states of the 3D system can be understood as the edge states of the 2D system on the surfaces which are parallel to the z -axis and therefore have a flat dispersion that does not depend on k_z [34]. This is analogous to the trivial or weak 3D topological insulators [1, 2]. In our case, due to the existence of spin-orbit coupling in all three spatial directions, the dispersion of the Majorana surface states is no longer flat. In this respect, the gapless topological FF superfluid is better regarded as the superfluid analogue of a strong topological insulator [1, 2], although the surface states may not have a Dirac-cone-like dispersion due to the gapless bulk.

Discussions. — Owing to their significant parameter space in the phase diagram, our proposed gapless topological FF superfluids could be easily detected in

current cold-atom experiments, where the isotropic or Rashba-type spin-orbit coupling can be engineered by using Raman lasers [29] or a sequence of pulsed inhomogeneous magnetic fields [30]. The unidirected Majorana surface modes, as a unique experimental evidence of the novel topological superfluid, could in principle be directly visible as arcs in momentum space at the Fermi surfaces in the momentum-resolved radio-frequency spectroscopy [37]. In solid-state systems, a promising candidate for realizing the gapless topological FF superfluid is to use a quantum well with large Rashba and Dresselhaus spin-orbit couplings (i.e., hole-doped InSb) in proximity to a conventional s -wave superconductor, where the in-plane Zeeman field in the quantum well layer can be controlled to minimize the orbital effect [38]. Other candidates include noncentrosymmetric superconductors such as CePt₃Si and Li₂Pd_xPt_{3-x}B [39], in the presence of a magnetic field on the plane of Rashba spin-orbit coupling.

In summary, we have proposed a new mechanism to create topologically non-trivial states by using an in-plane Zeeman field only. Novel gapless topological superfluids with inhomogeneous Fulde-Ferrell pairing order parameter can be realized using three-dimensional spin-orbit coupled s -wave superfluids, where the finite momentum pairing and topological order are both driven by the in-plane Zeeman field. They feature unidirected Majorana surface modes and a pair of zero-energy Majorana fermions at the edges, which are quite different from the standard gapped topological superfluids that are known to date. These new features will greatly enrich our understanding of topological quantum matters, in both solid-state and cold-atom systems.

Methods

Mean field theory. — The details of our theoretical framework have been presented in the previous work [20]. Here we give a brief summary. Taking the mean-field approximation for the pairing interaction term, the model Hamiltonian of the Fermi system can be rewritten into a compact form, $\mathcal{H} = (1/2) \int d\mathbf{r} \Phi^\dagger(\mathbf{r}) \mathcal{H}_{BdG}(\hat{\mathbf{k}}) \Phi(\mathbf{r}) - V\Delta^2/U_0 + \sum_{\mathbf{k}} (\xi_{\mathbf{k}+\mathbf{Q}/2} + \xi_{\mathbf{k}-\mathbf{Q}/2})/2$, where the explicit form of $\mathcal{H}_{BdG}(\hat{\mathbf{k}})$ in Eq. (2) is given by

$$\begin{bmatrix} \hat{\xi}_{\mathbf{k}+} + \lambda \hat{k}_z & \Lambda_{\mathbf{k}+}^\dagger & 0 & -\Delta \\ \Lambda_{\mathbf{k}+} & \hat{\xi}_{\mathbf{k}+} - \lambda \hat{k}_z & \Delta & 0 \\ 0 & \Delta & -\hat{\xi}_{\mathbf{k}-} + \lambda \hat{k}_z & \Lambda_{\mathbf{k}-} \\ -\Delta & 0 & \Lambda_{\mathbf{k}-}^\dagger & -\hat{\xi}_{\mathbf{k}-} - \lambda \hat{k}_z \end{bmatrix} \quad (6)$$

with $\hat{\xi}_{\mathbf{k}\pm} \equiv \hbar^2(\hat{\mathbf{k}} \pm \mathbf{Q}/2)^2/(2m) - \mu$ and $\Lambda_{\mathbf{k}\pm} \equiv \lambda(\hat{k}_x \pm q/2 + i\hat{k}_y) \pm h$. For a homogeneous Fermi gas with open boundary condition, the BdG Hamiltonian can be diagonalized by replacing the momentum operators \hat{k}_i

($i = x, y, z$) by the corresponding c -numbers k_i . Thus, we obtain the energy spectrum of Bogoliubov quasiparticles $E_{\eta\nu}(\mathbf{k})$, where $\nu \in (+, -)$ denotes the particle or hole branch and $\eta \in (1, 2)$ stands for the upper or lower helicity band. The mean-field thermodynamic potential Ω_{mf} at the temperature T can be written down straightforwardly,

$$\frac{\Omega_{\text{mf}}}{V} = \frac{1}{2V} \sum_{\mathbf{k}} \left[\xi_{\mathbf{k}+\mathbf{Q}/2} + \xi_{\mathbf{k}-\mathbf{Q}/2} - \sum_{\eta=1,2} E_{\eta+}(\mathbf{k}) \right] - \frac{\Delta^2}{U_0} - \frac{k_B T}{V} \sum_{\mathbf{k}\eta=1,2} \ln \left[1 + e^{-E_{\eta+}(\mathbf{k})/k_B T} \right], \quad (7)$$

where the last term is the standard expression of thermodynamic potential for non-interacting Bogoliubov quasiparticles. Due to the inherent particle-hole symmetry in the Nambu spinor representation, the summation over the quasiparticle energy has been restricted to the particle branch, to avoid double counting. For a given set of parameters (i.e., the temperature T , s -wave scattering length a_s etc.), different mean-field phases can be determined using the self-consistent stationary conditions: $\partial\Omega_{\text{mf}}/\partial\Delta = 0$, $\partial\Omega_{\text{mf}}/\partial q = 0$, as well as the conservation of total atom number, $n = -(1/V)\partial\Omega/\partial\mu$, where n is the number density. At a given temperature, the ground state has the lowest free energy $F = \Omega + \mu N$. For simplicity, we only report the results at zero temperature.

Majorana surface modes. — To determine the Majorana surface states in the topologically non-trivial phase, we impose a cylindrical hard wall potential, for example, perpendicular to the y - z plane, so that any single-particle wavefunction must vanish identically at the boundary $r = L$. We assume that the radius is sufficiently large so that we can use the solution of a uniform pairing gap. Accordingly, in the BdG Hamiltonian Eq. (6), we replace the momentum operator k_y and k_z with its corresponding derivatives in cylindrical coordinates where longitudinal axis is chosen along x -direction. It can be diagonalized by using the following ansatz for the Bogoliubov wavefunctions,

$$\begin{bmatrix} u_{\uparrow}(\mathbf{r}) \\ u_{\downarrow}(\mathbf{r}) \\ v_{\uparrow}(\mathbf{r}) \\ v_{\downarrow}(\mathbf{r}) \end{bmatrix} = \frac{e^{im\theta}}{\sqrt{2\pi}} \sum_{n=1}^{N_{\text{max}}} \begin{bmatrix} \frac{J_m(\kappa_n^{(m)} r/L) u_{n\uparrow}}{\sqrt{\mathcal{N}_n^{(m)}}} \\ \frac{J_{m+1}(\kappa_n^{(m+1)} r/L) e^{i\theta}}{\sqrt{\mathcal{N}_n^{(m+1)}}} u_{n\downarrow} \\ \frac{J_{m+1}(\kappa_n^{(m+1)} r/L) e^{i\theta}}{\sqrt{\mathcal{N}_n^{(m+1)}}} v_{n\uparrow} \\ \frac{J_m(\kappa_n^{(m)} r/L) v_{n\downarrow}}{\sqrt{\mathcal{N}_n^{(m)}}} \end{bmatrix} e^{ik_x x} \quad (8)$$

where $\kappa_n^{(m)}$ is the n th positive root of Bessel function of the first kind $J_m(\rho)$ with $m \geq 0$. For states with $m < 0$, we have instead $J_{-m}(\rho) = (-1)^m J_m(\rho)$. Orthogonal condition is given by $\int_0^L J_m(\kappa_n^{(m)} r/L) J_m(\kappa_l^{(m)} r/L) r dr = 0$ where integer $n \neq l$ and normalization reads as $\mathcal{N}_n^{(m)} = \int_0^L J_m(\kappa_n^{(m)} r/L) J_m(\kappa_n^{(m)} r/L) r dr = \frac{1}{2} L^2 [J_{m+1}(\kappa_n^{(m)})]^2$.

Inserting this ansatz into the BdG equation, we convert the BdG Hamiltonian into a $4N_{\text{max}}$ by $4N_{\text{max}}$ Hermitian matrix,

$$\mathcal{H}_{11n}^{(m)} u_{n\uparrow} - i\lambda \sum_{l=1}^{N_{\text{max}}} \mathcal{W}_{ln}^{(m)} u_{l\downarrow} - \Delta v_{n\downarrow} = E_{k_x}^{(m)} u_{n\uparrow} \quad (9)$$

$$i\lambda \sum_{l=1}^{N_{\text{max}}} \mathcal{W}_{nl}^{(m)} u_{l\uparrow} + \mathcal{H}_{22n}^{(m)} u_{n\downarrow} + \Delta v_{n\uparrow} = E_{k_x}^{(m)} u_{n\downarrow} \quad (10)$$

$$\Delta u_{n\downarrow} + \mathcal{H}_{33n}^{(m)} v_{n\uparrow} + i\lambda \sum_{l=1}^{N_{\text{max}}} \mathcal{W}_{nl}^{(m)} v_{l\downarrow} = E_{k_x}^{(m)} v_{n\uparrow} \quad (11)$$

$$-\Delta u_{n\uparrow} - i\lambda \sum_{l=1}^{N_{\text{max}}} \mathcal{W}_{ln}^{(m)} v_{l\uparrow} + \mathcal{H}_{44n}^{(m)} v_{n\downarrow} = E_{k_x}^{(m)} v_{n\downarrow} \quad (12)$$

where all the matrix elements have been analytically worked out (not shown here). The diagonalization directly gives rise to the energies and wavefunctions of the Majorana surface states.

-
- [1] Hasan, M. Z. & Kane, C. L. Topological insulators. *Rev. Mod. Phys.* **82**, 3045 (2010).
 - [2] Qi, X.-L. & Zhang, S.-C. Topological insulators and superconductors. *Rev. Mod. Phys.* **83**, 1057 (2011).
 - [3] Nayak, C., Simon, C. H., Stern, A., Freedman, M. & Das Sarma, S. Non-abelian anyons and topological quantum computation. *Rev. Mod. Phys.* **80**, 1083 (2008).
 - [4] Wilczek, F. Majorana returns. *Nature Phys.* **5**, 614-618 (2009).
 - [5] Read, N. & Green, D. Paired states of fermions in two dimensions with breaking of parity and time-reversal symmetries and the fractional quantum Hall effect. *Phys. Rev. B* **61**, 10267 (2000).
 - [6] Moore, G. & Read, N. Nonabelions in the fractional quantum hall effect. *Nucl. Phys. B* **360**, 362-396 (1991).
 - [7] Fu, L. & Kane, C. L. Superconducting Proximity effect and Majorana fermions at the surface of a topological insulator. *Phys. Rev. Lett.* **100**, 096407 (2008).
 - [8] Sau, J. D., Lutchyn, R. M., Tewari, S. & Das Sarma, S. Generic new platform for topological quantum computation using semiconductor heterostructures. *Phys. Rev. Lett.* **104**, 040502 (2010).
 - [9] Oreg, Y., Refael, G. & von Oppen F. Helical liquids and Majorana bound states in quantum wires. *Phys. Rev. Lett.* **105**, 177002 (2010).
 - [10] Zhang, C., Tewari, S., Lutchyn, R. M. & Das Sarma, S. $p_x + ip_y$ superfluid from s -wave interactions of fermionic cold atoms. *Phys. Rev. Lett.* **101**, 160401 (2008).
 - [11] Sato, M., Takahashi, Y., & Fujimoto S. Non-abelian topological order in s -wave superfluids of ultracold fermionic atoms. *Phys. Rev. Lett.* **103**, 020401 (2009).
 - [12] Mourik, V., Zuo, K., Frolov, S. M., Plissard, S. R., Bakkers, E. P. A. M. & Kouwenhoven, L. P. Signatures of Majorana fermions in hybrid superconductor-semiconductor nanowire devices. *Science* **336**, 1003-1007 (2012).

- [13] Williams, J. R., Bestwick, A. J., Gallagher, P., Hong, S. S., Cui, Y., Bleich, A. S., Analytis, J. G., Fisher, I. R. & Goldhaber-Gordon, D. Unconventional Josephson effect in hybrid superconductor-topological insulator devices. *Phys. Rev. Lett.* **109**, 056803 (2012).
- [14] Rokhinson, L. P., Liu, X. & Furdyna, J. K. The fractional a.c. Josephson effect in a semiconductor-superconductor nanowire as a signature of Majorana particles. *Nature Phys.* **8**, 795-799 (2012).
- [15] Dong, L., Jiang, L., Hu, H. & Pu, H. Finite-momentum dimer bound state in a spin-orbit-coupled Fermi gas. *Phys. Rev. A* **87**, 043616 (2013).
- [16] Shenoy, V. B. Flow-enhanced pairing and other unusual effects in Fermi gases in synthetic gauge fields. *Phys. Rev. A* **88**, 033609 (2013).
- [17] Zheng, Z., Gong, M., Zou, X., Zhang, C. & Guo, G.-C. Route to observable Fulde-Ferrell-Larkin-Ovchinnikov phases in three-dimensional spin-orbit-coupled degenerate Fermi gases. *Phys. Rev. A* **87**, 031602(R) (2013).
- [18] Wu, F., Guo, G.-C., Zhang, W. & Yi, W. Unconventional superfluid in a two-dimensional Fermi gas with anisotropic spin-orbit coupling and Zeeman fields. *Phys. Rev. Lett.* **110**, 110401 (2013).
- [19] Liu, X.-J. & Hu, H. Inhomogeneous Fulde-Ferrell superfluidity in spin-orbit-coupled atomic Fermi gases. *Phys. Rev. A* **87**, 051608(R) (2013).
- [20] Dong, L., Jiang, L. & Pu, H. Fulde-Ferrell pairing instability in spin-orbit coupled Fermi gas. *New J. Phys.* **15**, 075014 (2013).
- [21] Hu, H. & Liu, X.-J. Fulde-Ferrell superfluidity in ultracold Fermi gases with Rashba spin-orbit coupling. *New J. Phys.* **15**, 093037 (2013).
- [22] Qu, C., Zheng, Z., Gong, M., Xu, Y., Mao, L., Zou, X., Guo, G. & Zhang, C. Topological superfluids with finite momentum pairing and Majorana fermions. *Nat. Commun.* **4**, 2710 (2013).
- [23] Zhang, W. & Yi, W. Topological Fulde-Ferrell-Larkin-Ovchinnikov states in spin-orbit-coupled Fermi gases. *Nat. Commun.* **4**, 2711 (2013).
- [24] Fai, C. C. & Ming G. Pairing symmetry, phase diagram and edge modes in topological Fulde-Ferrell-Larkin-Ovchinnikov phase. *ArXiv e-print* (2013) <http://arxiv.org/abs/1312.3000>
- [25] Fulde P. & Ferrell, R. A., Superconductivity in a strong spin-exchange field. *Phys. Rev.* **135**, A550-A563 (1964).
- [26] Lin, Y.-J., Jiménez-García, K. & Spielman, I. B. Spin-orbit coupled Bose-Einstein condensates. *Nature* **471**, 83-86 (2011).
- [27] Wang, P., Yu, Z.-Q., Fu, Z., Miao, J., Huang, L., Chai, S., Zhai, H. & Zhang, J. Spin-orbit coupled degenerate Fermi gases. *Phys. Rev. Lett.* **109**, 095301 (2012).
- [28] Cheuk, L. W., Sommer, A. T., Hadzibabic, Z., Yefsah, T., Bakr, W. S. & Zwierlein, M. W. Spin-injection spectroscopy of a spin-orbit coupled Fermi gas. *Phys. Rev. Lett.* **109**, 095302 (2012).
- [29] Anderson, B. M., Juzeliūnas, G., Galitski, V. M. & Spielman, I. B. Synthetic 3D spin-orbit coupling. *Phys. Rev. Lett.* **108**, 235301 (2012).
- [30] Anderson, B. M., Spielman, I. B. & Juzeliūnas, G. Magnetically generated spin-orbit coupling for ultracold atoms. *Phys. Rev. Lett.* **111**, 125301 (2013).
- [31] Wan, X., Turner, A. M., Vishwanath, A. & Savrasov, S. Y. Topological semimetal and Fermi-arc surface states in the electronic structure of pyrochlore iridates. *Phys. Rev. B* **83**, 205101 (2011).
- [32] Burkov, A. A. & Balents, L. Weyl semimetal in a topological insulator multilayer. *Phys. Rev. Lett.* **107**, 127205 (2011).
- [33] Xu, G., Weng, H., Wang, Z., Dai, X. & Fang Z. Chern semimetal and the quantized anomalous Hall effect in HgCr_2Se_4 . *Phys. Rev. Lett.* **107**, 186806 (2011).
- [34] Sau, J. D. & Tewari, S. Topologically protected surface Majorana arcs and bulk Weyl fermions in ferromagnetic superconductors. *Phys. Rev. B* **86**, 104509 (2012).
- [35] Xu, Y., Chu, R. & Zhang, C. Anisotropic Weyl fermions from the quasiparticle excitation spectrum of a 3D Fulde-Ferrell superfluid. *Phys. Rev. Lett.* **112**, 136402 (2014).
- [36] Schnyder, A. P., Ryu, S., Furusaki, A. & Ludwig, A. W. W. Classification of topological insulators and superconductors in three spatial dimensions. *Phys. Rev. B* **78**, 195125 (2008).
- [37] Liu, X.-J., Jiang, L., Pu, H. & Hu, H. Probing Majorana fermions in spin-orbit-coupled atomic Fermi gases. *Phys. Rev. A* **85**, 021603(R) (2012).
- [38] Alicea, J. Majorana fermions in a tunable semiconductor device. *Phys. Rev. B* **81**, 125318 (2010).
- [39] Schnyder, A. P. & Ryu, S. Topological phases and surface flat bands in superconductors without inversion symmetry. *Phys. Rev. B* **84**, 060504(R) (2011).

Acknowledgement HH and XJL were supported by the ARC Discovery Projects (Grant Nos. FT130100815, DP140103231 and DP140100637) and NFRP-China (Grant No. 2011CB921502). HP was supported by the NSF, the Welch Foundation (Grant No. C-1669) and the DARPA OLE program.

Author contributions HH, HP and XJL conceived the concept of topological superfluidity induced by an in-plane Zeeman field. HH, LD and XJL performed numerical calculations. YC checked the topological superfluidity in the case of two-dimensional atomic Fermi gases. All authors contributed to the writing of the manuscript. Correspondence and requests for numerical data should be addressed to X.-J. Liu (email: xiajiliu@swin.edu.au).

Competing financial interests The authors declare no competing financial interests.

Supplementary information

Here we discuss the Majorana surface states with a hard wall potential along a specific direction, say, along the y -direction. Any single-particle wavefunction must vanish identically at the boundary $y = 0$ or $y = L$. We assume that the length L is sufficiently large so we use the solution of a uniform pairing gap. Accordingly, in the BdG Hamiltonian Eq. (6), we replace the momentum operator k_y with $-i\partial_y$. It can be diagonalized by using

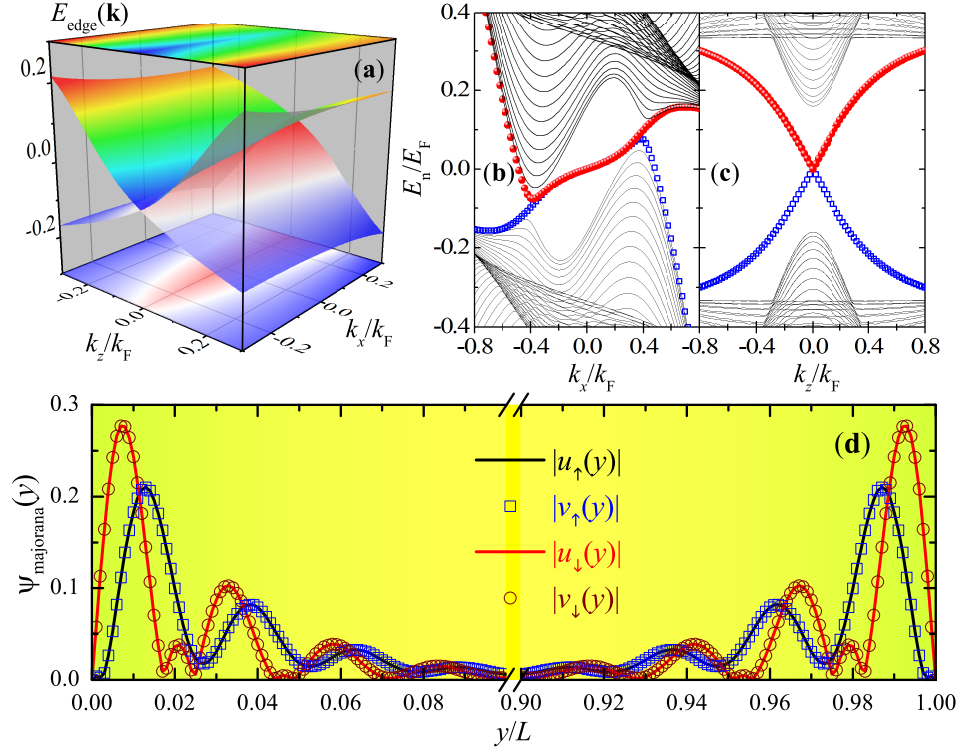


FIG. 5: (Color online) **Majorana surface states arising from the hard wall confinement along the y -direction.** (a) The surface state dispersion forms two sheets which cross at the line $k_z = 0$. (b) and (c) The full energy spectrum $E_{2\pm}(k_x, k_z)$ along the k_z or k_x axis, respectively. The surface states at the two boundaries are highlighted by red solid circles and blue empty squares, respectively. (d) The wavefunction of the zero-energy Majorana fermions at $k_x = 0$ and $k_z = 0$. In numerical calculations, we have set the length of the confinement $L = 200k_F^{-1}$. Other parameters are $\lambda = E_F/k_F$ and $h = 0.4E_F$ as in Fig. 4.

the following ansatz for the Bogoliubov wavefunctions,

$$u_{\sigma}(y) = \sum_{n=1}^{N_{\max}} u_{n\sigma} \psi_n(y), \quad (13)$$

$$v_{\sigma}(y) = \sum_{n=1}^{N_{\max}} v_{n\sigma} \psi_n(y), \quad (14)$$

where $\psi_n(y) = \sqrt{2/L} \sin[n\pi y/L]$ is the eigenfunction of the hard wall potential with eigenvalue $\epsilon_n = \hbar^2 n^2 \pi^2 / (2mL^2)$. Inserting this ansatz into the BdG equation, we convert the BdG Hamiltonian into a $4N_{\max}$ by $4N_{\max}$ symmetric matrix, whose diagonalization directly leads to the energies and wavefunctions of the Majorana surface states.

With this hard wall confinement, the dispersion of Majorana surface states is shown in Fig. 5. In momentum space, k_x and k_z are still good quantum numbers, so we actually plot $\min E_{2+}(k_x, k_z)$ and $\max E_{2-}(k_x, k_z)$. There are two sheets in the energy dispersion (Fig. 5a), corresponding to the surface states localized at the boundary $y = 0$ and $y = L$, respectively. Remarkably, these two sheets cross at the line $k_z = 0$, indicating that along this line the two branches of surface

states are unidirected, that is, propagating in the same direction on opposite boundaries. This is highlighted in Fig. 5b, from which we also identify that the unidirected Majorana surface states smoothly connect the two Weyl nodes $(\pm k_W, 0, 0)$ in the bulk, where $k_W \simeq 0.4k_F$. Recall that at equilibrium there are no net atomic currents. As in the cylindrically symmetric case, the current due to these co-propagating surface states on opposite boundaries therefore must be compensated by the current induced by some extra counter-propagating modes in the bulk. This can only happen in systems with a gapless bulk. We note that, the unidirected Majorana surface states only occur along the line $k_z = 0$. Actually, if we make a cut on the two sheets along other directions, for example, along the line $k_x = 0$, it is easy to see that the Majorana surface states become counter-propagating (see Fig. 5c for the dispersion as a function of k_z), resembling the surface states in the standard gapped topological superfluid. This follows the fact that at $k_x = 0$ our topological FF superfluid is actually gapped in the bulk. By comparing the two limiting cases shown in Figs. 5b and 5c, it is clear that the unidirected surface states discussed in our work is a unique feature of novel gapless topological FF superfluid.